The copyright of this thesis vests in the author. No quotation from it or information derived from it is to be published without full acknowledgement of the source. The thesis is to be used for private study or non-commercial research purposes only.

Published by the University of Cape Town (UCT) in terms of the non-exclusive license granted to UCT by the author.

University of Cape Town

Maxima in strangeness observed in heavy ion collisions using statistical models

Nawahl Razak

University of Cape Town

A thesis submitted in fulfilment of the requirements
for the degree of Master of Science
in the Department of Physics
University of Cape Town

June 2004

UT 530 RAZA
762732

University of Cape Town

Contents

University of Cape Town

University of Cape Town

List of Figures

University of Cape Town

University of Cape Town

Chapter 1

Introduction

Nucleus-Nucleus collisions enable the heating and compression of nuclei in order to probe matter under extreme temperature and energy density. With a resonance gas model of hadronic matter, Hagedorn [1] came to the conclusion that on increasing the energy density, hadronic matter could not exist above a limiting temperature of approximately 160 MeV. Above this temperature it is expected that hadronic matter undergoes a phase transition to a state of deconfined fundamental quarks and gluons known as a quark gluon plasma (QGP).

The big bang theory of the origin of the universe suggests that at some very early time (of the order of a microsecond after the big bang) in the history of our known universe, the extreme temperatures and densities required for the existence of a QGP were met. By colliding nuclei, we are in fact simulating conditions (on a much smaller scale) of the big bang, so that the state of matter which might have existed in the early universe (and which possibly still exists in the inner core of neutron stars) can be studied.

By varying the collision energy and the size of the colliding nuclei, it is possible to vary the degree of heating and compression. In doing so we are able to explore various regions of the phase diagram of hadronic matter (figure 1) experimentally. In the low temperature and baryon density region, quarks and gluons are confined inside hadrons in accordance with the standard model of particle physics. In this region, right-left chiral symmetry is spontaneously broken. At high temperatures and nuclear densities, quarks are liberated and chiral symmetry restored. It is

University of Cape Town

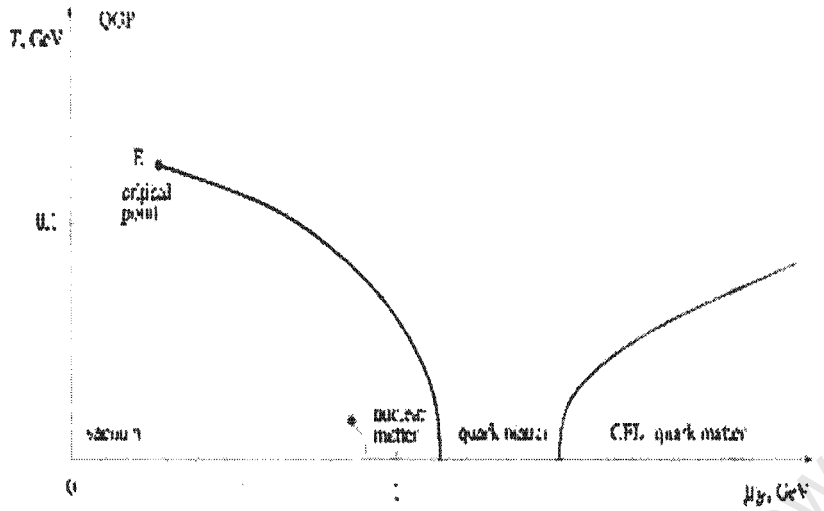

Figure 1.1: Phase diagram of hadronic matter [2].

also expected that in the high baryon density and low temperature range, pairing up of quarks would lead to the breaking of color symmetry. The resulting phase should behave analogously to a superconducting phase. In figure 2.3 the experimental points, which map out the region of the phase diagram explored by heavy ion collisions, are shown. The main goal of high energy experiments is to study the expected transition from ordinary nuclear matter to a QGP. Knowledge of the dynamics of this phase transition could possibly even lead to us to understand the origin of the observed large scale inhomogenous features (like clusters of galaxies) in our universe.

To date there is no precise theory available for interpretating experimental results. Quantum Chromodynamics (QCD), the theory describing the strong interaction of quarks by the exchange of gluons, exhibits a strong long range behavior. This at the moment poses the limitation on the QCD theory because calculations can only be performed perturbatively. Phenomenology is practically the only means available. Statistical models have been widely used in this respect. Despite their simplicity, they have been very successful in reproducing and predicting properties of matter produced in collisions at relativistic energies. Inevitably models attempting to describe matter in the various stages of collisions are centered

University of Cape Town

around properties which are suggestive of unique behaviour of matter under extreme conditions.

1.1 Heavy Ion Collisions

In the center of mass frame of two colliding nuclei (figure 1.2), they appear strongly Lorentz contacted. The interacting nucleons (from both target and projectile nucleons) are called participants while the non-interacting nucleons which proceed almost unaffected are known as spectators. The impact parameter b is a measure of the overlap between the target and projectile nucleons.

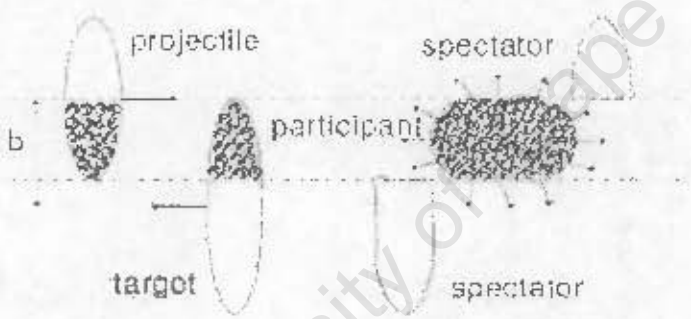

Figure 1.2: Schematic diagram of a collision of two nucleons in the center of mass frame.

University of Cape Town

At facilities like the AGS (Alternating Gradient Synchrotron) and the RHIC (Relativistic Heavy Ion Collider) at Brookhaven National Laboratory near New York as well as the SPS (Super Proton Synchrotron) at CERN in Geneva, heavy ions are accelerated up to hundreds of GeV per nucleon. Here experiments have been performed over a wide energy range. The percentage of kinetic energy lost (referred to as stopping) by the participant nucleons (in the c.m frame) in these collisions determine the resulting energy and particle density. High baryon density is achieved by colliding nuclei at energies where they very nearly stop one another and the number of produced particles is low. This is the case at the AGS. At higher collision energy (such as at the SPS), lower baryon density with

correspondingly higher energy density is achieved. RHIC collisions (where collision energy is roughly ten times higher that at the SPS), extremely high energy density is achieved with baryon density close to zero.

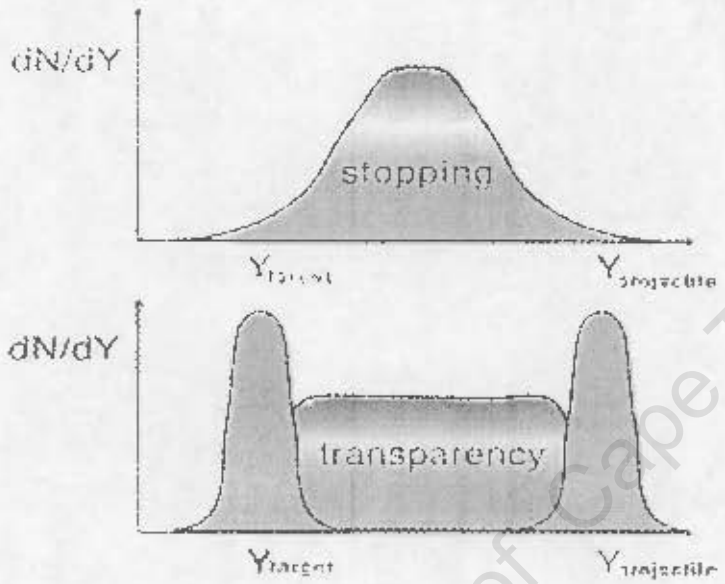

Figure 1.3: Rapidity distributions of baryons in the two extreme cases: complete stopping (top) and complete transparency (bottom)[3].

University of Cape Town

The central region mimics the hot vaccuum of the early universe. The amount of stopping in a collision can be seen experimentally by looking at the rapidity distribution of baryons (see figure 1.3). Under a Lorentz boost, rapidity is shifted by a constant amount so that the differences in rapidity between particles and the shape of the rapidity distributions are preserved. Rapidity is given by

$$y = \frac{1}{2} \log \frac{E + P_z}{E - P_z} \tag{1.1}$$

where E is the energy of the particle, and P_z it's momentum along the beam direction.

1.1.1 Evolution of the colliding system

QCD predicts that if the energy and baryon density (resulting from the collision) in the central region exceed certain critical values, a QGP should be formed. This state is expected to live for a very short time (of the order of $10^{-22}s$). The QGP should cool rapidly and undergo a phase transition to hadrons. Inelastic collisions among the hadrons proceed until chemical freezeout. After chemical freezeout particle yields remain unchanged. The observed hadron yields provide valuable information about chemical freezeout. Even after chemical freezeout, elastic collisions proceed, redistributing the total momentum throughout the hadronic constituents in the system. Thermal freezeout occurs when inelastic collisions cease. Studying the observed momentum distributions, provides informations about thermal freezeout.

1.2 QGP Signals

The size and lifetime of a QGP created in heavy ion collisions are both expected to be very small. Therefore, establishing the formation of a QGP amounts to identifying experimental observables present in the final hadronic state which could indicate properties of the hadronic phase resulting solely from the formation of a QGP. Such signals should originate during initial stages of the collision and remain unaltered during further evolution of the system. Several (otherwise) plausible QGP signals are clouded by backround from the hot hadronic gas or modified by final state processes in the hadronic phase. Some of the dely discussed signals of a QGP formation are presented below.

University of Cape Town

1.2.1 Direct Photons

Photons and lepton pairs originating in the QGP are direct QGP probes [4, 5]. They are weakly interacting probes which decouple from the hot phase of matter formed in the initial stages of the collision. They do not interact with the subsequently created surrounding matter once they are produced and should therefore emerge at the observable hadronic stage as virtually unaltered thermal radiation with direct information of the earlier state. A rapid change in the lepton pair

spectrum has been suggested to be an indication of a deconfinement transition [6].

1.2.2 Heavy quarkonium suppression

Heavy quark pairs (which form quarkonia) are produced in relativistic heavy ion collisions on time scales of the order of $1/2m$, where m is the mass of the heavy quark. The pair forms a physical resonance over some formation time, traversing the medium in which it was created, then finally leaving the interacting system and decaying into a dimuon which can then be detected.

The suppression of heavy quarkonium states such as ($c\bar{c}$ and $b\bar{b}$) has been suggested (based on colour screening) nearly two decades ago my Matsui and Satz as a signaure of the phase transition to deconfined matter (QGP) in heavy ion collisions [7]. Debye screening of quark matter [8] suggests that increasing the energy density in heavy ion collisions leads to a reduction in the range of the strong force (which is inversely proportional to the density of colour charges). Beyond some threshold, the range of the strong force is reduced to the extent that quarks inside quarkonium resonances seperate and appear at hadronization in other resonances with open charm and beauty. The high binding energy of the J/Ψ ($c\bar{c}$) and Υ ($b\bar{b}$) states indicates that hard gluons present in a QGP have enough momentum to lead to the dissociation of these quarkonium states. Thus the suppression of quarkonium states is characteristically related to the presence of a QGP. Additional processes such as the decay of the B meson and $D\bar{D}$ states counteract the expected suppression. It is important to filter out the contribution of these decays in order to observe heavy quarkonium suppression.

University of Cape Town

1.2.3 Jet quenching

Jet quenching may serve as another useful mean of identifying the formation of a QGP. Pairs of very energetic quarks and gluons are created in heavy ion collisions. These energetic particles end up as jets of highly energetic hadrons. By observing the energy loss of the jets through the medium (which results from a heavy ion collision) it is possible to infer the density of the medium traversed by

the jet [9, 10]. Jet quenching has been observed at RHIC. Here it was concluded that a very dense medium was created [11]. It remains to determine whether this medium was QGP or not.

1.2.4 Charge fluctuations

Event by even fluctuations in charge have also been suggested as a possible signal of QGP formation [12]. The reasoning is as follows: In hadronic matter, the unit of charge is 1 whereas the unit of charge in a QGP is 1/3. Although overall charge is not affected, the fluctuations in charge would be since this quantity is dependent on the square of the unit of charge which as one would expects would be very different for a QGP and hadronic matter. Fluctuations in charge can be studied by looking at ratios of certain charged particles.

1.2.5 Enhancement of Strangeness

A high gluon density is present in a QGP as a result of colour bonds being broken. The gluon component of the QGP is able to produce pairs of $s\bar{s}$ quarks very rapidly [13]. This leads to the expectation that strangeness would be significantly enhanced if a QGP was created. In particular, the high strangeness density should lead to the enhanced formation of multistrange hadrons [14] which are rarely produced in hadronic collisions [15, 16]. In addition, it is expected that the enhancement of multistrange baryons should follow the hierachy $\Omega > \Xi > \Lambda$. The enhancement of multistrange baryons should increase with strangeness content of the particle.

1.3 Overview of Strangeness

1.3.1 Introduction to Strangeness

Strange particle production has proved to be very useful in the study of relativistic heavy ion collisions. For several decades, the study of how strange hadrons

University of Cape Town

might help with understanding the nature of matter, has received considerable attention. A wide variety of strange particles is observed at the hadronization stage in these collisions. They decay (into a cascade of hadrons) over a range of several centimeters via the weak interaction. This is represented in figure 1.4. By applying basic conservation laws to the resulting decay cascade, the original 'strange' parent particle can be reconstructed in a relatively straightforward way.

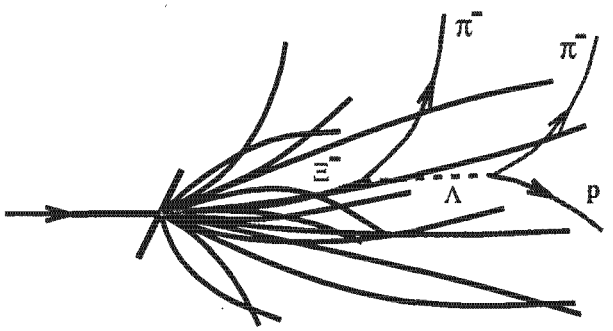

Figure 1.4: Illustration of a Ξ^- cascade decay [17].

In a hadronic medium, $s\bar{s}$ pairs are produced via inelastic scattering of hadrons. Further inelastic scattering results in the formation of hadrons containing strange quarks (and antiquarks). In a QGP, the high gluon density and low energy threshold for the dominant QCD processes of $s\bar{s}$ formation implies that strangeness should be efficiently produced and equilibrated. In a QGP, the interaction between quarks and gluons occurs within a volume much larger than the size of a nucleus, and thus the processes of $q\bar{q} \rightarrow s\bar{s}$ and $gg \rightarrow s\bar{s}$ occur more frequently. The s and $\bar{s}$ quarks are able to traverse the QGP independently of each other, interacting with other constituents in the plasma. These quarks are eventually observed in resonances containing s and $\bar{s}$ quarks after hadronization (see figure 1.5).

In the QGP phase, the process of thermal gluon fusion ($gg \rightarrow s\bar{s}$) is expected to be the dominant contributor (by an overwhelming amount) to the formation of $s\bar{s}$ pairs. Thus the enhancement of strangeness (observed at hadronization as enhancement of strange hadrons) would be indicative of the presence of thermal

University of Cape Town

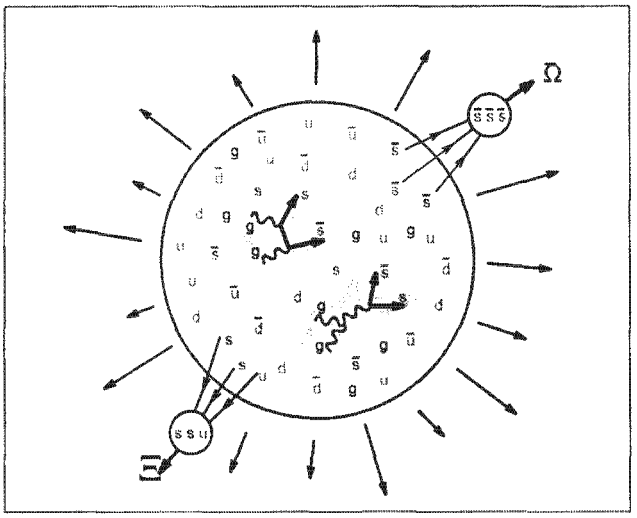

Figure 1.5: Illustration the formation of strange hadrons from a QGP. Gluon fusion into strangeness followed by hadronization due to recombination in the QGP is also shown in inserts [17].

gluons which in turn indicates the formation of a deconfined phase of quarks and gluons.

The above discussion lead to the following specific expected observations of strangeness enhancement [18, 19]. Firstly, strangeness enhancement on a fundamental level could be reflected in the global strangeness enhancement of strangeness from $p+p$ to $p+A$ to $A+A$ collisions. Secondly, the enhancement in production of multistrange baryons and antibaryons. In addition, a QGP formed close to chemical equilibrium is expected to undergo a phase transition to a population of hadrons close to chemical equilibrium.

1.3.2 Global Strangeness enhancement

At CERN SPS, strangeness enhancement was observed from $p+p$ to $p+A$ to $A+A$ collisions [20, 21, 22]. There is an enhancement by a factor of 2 in go-

University of Cape Town

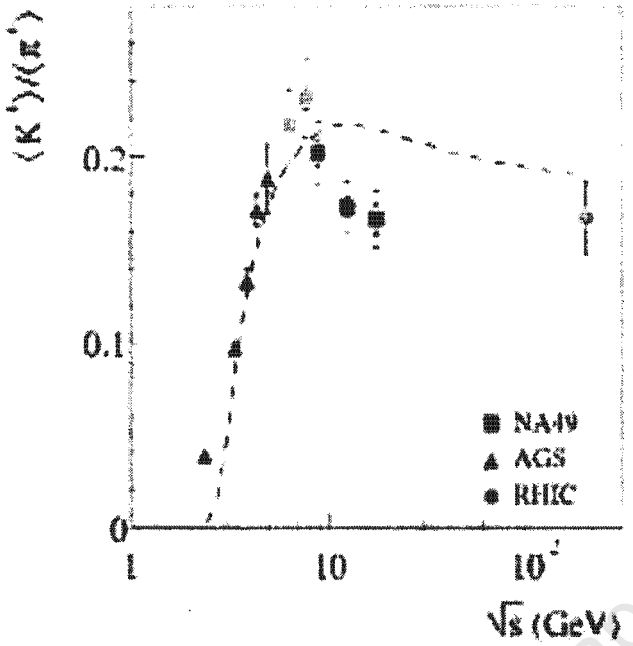

Figure 1.6: Fully integrated K^+/π^+ ratio measured in heavy ion collisions at various collision energies. The dashed line is a thermal model prediction. [24].

ing from $p + p$ to heavy ion collisions. This can be seen in figure 1.6 in the K^+/π^+ ratio. This substantial enhancement is a unique property to heavy ion collisions. Within a canonical statistical description, this is explained in terms of suppression of phase space [23] available to small systems of strange particles due to strangeness conservation. The canonical treatment is necessary for p+p interactions since only a few strange particles are produced.

In relativistic $A + A$ collisions, enough strange particles are produced so that a grand canonical statistical description is adequate. Thus from a statistical viewpoint, the enhancement observed from $p + p$ to $A + A$ collisions appears as a consequence of the transition from the canonical to the grand canonical regime. Global strangeness enhancement is therefore not necessarily the result of deconfinement.

University of Cape Town

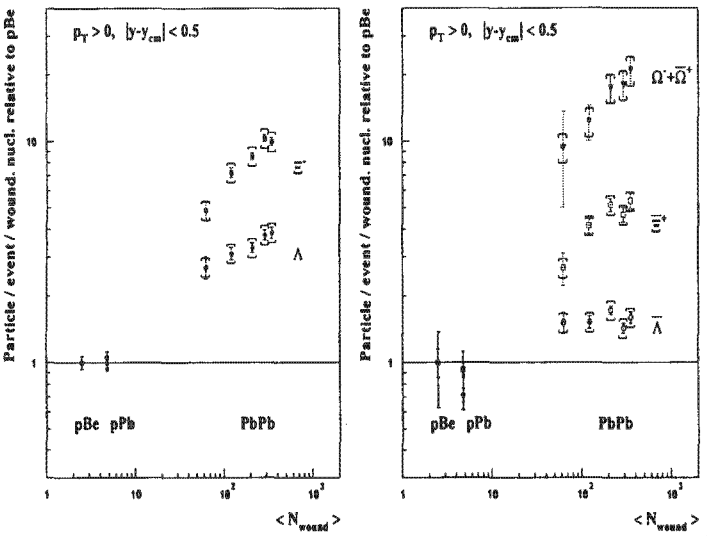

Figure 1.7: Strange particle yields per participant at mid-rapidity normalized to $p + Be$ collisions from data obtained by NA57 at SPS [22] collaboration [25].

1.3.3 Multistrange Baryons

Data from the WA97 and NA57 on antihyperon yields indicate that strangeness enhancement is increasing with the strangeness content of the particle. This can be seen in figure 1.7 which shows the yield per participant in $Pb-Pb$ relative to $p-Be$ and $p-Pb$ collisions. In addition, the NA57 data shows an abrupt change of the $\bar{\Xi}$ enhancement for lower centrality. This has been suggested as possibly signalling the onset of new dynamics.

A combination of microscopic transport models, and pre-hadronic mechanisms partially explain the enhancement pattern observed in multistrange hadrons for the most central collisions. However, microscopic transport models fail to reproduce their centrality dependence. The basic features of the WA97 data on multistrange particle enhancement was shown to be reproducible with the canonical statistical model [27]. This is shown in figure 1.8.

University of Cape Town

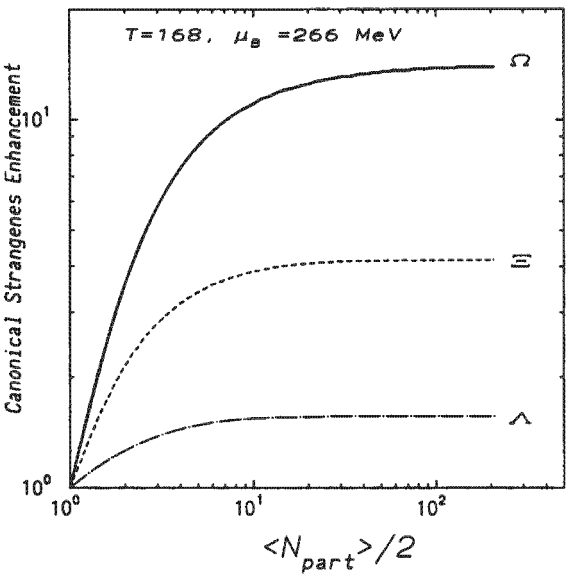

Figure 1.8: Particle multiplicities per participant normalized to its value in $p+p$ system as a function of A_{part} calculated in a canonical statistical model [27]

1.4 Objectives

Strangeness enhancement as discussed above is not sufficient to identify a QGP. The non-monotonic behavior of strangeness as a function of centrality or collision energy has been suggested as an alternative signal of QGP formation. This proposal motivated the energy scan program at the CERN SPS [28]. Indeed, maxima in strange to non-strange particle ratios has been observed experimentally.

The aim of my thesis is to investigate the maximum in relative strangeness evident in experimental strange to non strange particle ratios. In chapter 2, I provide a description of the framework of the thermal model with reference to the strangeness maximum. Here I also investigate the interesting correlation between the appearance of the maximum (as predicted by the thermal model) and experimental conditions at chemical freezeout. The statistical model of the early stages (SMES) - developed by Marek Gaździcki - among other things, also provides a means of predicting the maximum in relative strangeness differently to the thermal model. I provide a review of the framework of this model in chapter 3, specifically concentrating on how the model predicts the maxima in relative

University of Cape Town

strangeness. Since the thermal model and SMES are inherently different, I provide, in chapter 4, a comparison the two models. Here I concentrate on what specific features in each model is responsible for their respective predictions of the maximum.

University of Cape Town

University of Cape Town

Chapter 2

The Thermal Model

2.1 Overview of the model

Statistical thermodynamics has for a long time played an important role in the study of the behavior of strongly interacting matter. Hadron multiplicities calculated using thermal models, agree well with the experimentally observed hadron multiplicities.

In handling baryon number and strangeness and electric charge conservation, there is a choice of the following statistical formalisms: Grand Canonical, Canonical and Mixed Canonical. When the amount of particles containing the conserved quantities are large, the introduction of chemical potentials in the grand canonical ensemble is sufficient to handle the conserved quantities. This is adequate for the description of heavy ion collisions at relativistic energies. On the other hand, in elementary particle collisions, very few particles containing the conserved quantities are produced. Thus conservation needs to be applied exactly. The Canonical formalism is appropriate in this case. In heavy ion collisions at low energy a mixed canonical treatment is needed. Baryon number and electric charge conservation can be handled grand canonically (a large number of baryons and charged particles are present) whereas strangeness is treated canonically (particles carrying strangeness are not produced in abundance). For my purpose grand canonical treatment is sufficient.

University of Cape Town

2.2 The grand canonical ensemble

In the collisions of heavy ions at relativistic energies, particles are created from kinetic energy. As a result, particle number is not conserved in the usual sense. Instead, the main interest lies in the conserved quantum numbers baryon number B, strangeness S and electric charge Q. If the temperature and volume are large enough, particle creation is commonly described using this ensemble where conservation of quantum numbers is ensured by the introduction of the appropriate chemical potential (μ_B, μ_S and μ_Q) for each conserved quantum number. The grand canonical ensemble is however only effective if the number of particles carrying the conserved quantum number is large. If the number of particles is small, charge conservation must be handled exactly and locally within the canonical framework.

The grand canonical partition function is given by

$$Z_{GC}(T, V, \mu) \equiv Tr\left[e^{-\frac{1}{T}(H-\mu_j Q_j)}\right] \tag{2.1}$$

where H is the Hamiltonian describing the system, Q_j refers to the conserved charges in the system and μ_j is the chemical potential which ensures that the charge Q_j is conserved on average.

For a hadron resonance gas containing i different hadrons, the partition function is the product of the partition functions of each type, so that

$$\ln Z\,(T, V, \mu) = \sum_i \ln Z_i\,(T, V, \mu) \tag{2.2}$$

The Hamiltonian is described by the hadronic gas containing contributions from hadrons with a mass below $\sim 2\ GeV$. The hadronic spectrum for this mass range and decay properties of resonances are taken from the PDG booklet. This limit on hadron mass however only holds for temperatures below 190 MeV. Above this temperature, higher mass resonances, contribute significantly to the hadronic spectrum and as yet, there is not enough information about them available . The introduction of chemical potentials ensures quantum number conservation on average by allowing fluctuations about average values.

University of Cape Town

For particle i with degeneracy g_i, baryon number B_i, strangeness S_i and electric charge Q_i one has

$$\ln Z_i = \pm \frac{V g_i}{2\pi^2} \int_0^\infty p^2 dp \ln \left[1 \pm \lambda_i \exp\left(-E_i/T\right)\right] \tag{2.3}$$

The $+$ refers to fermions and the $-$ to bosons. The fugacity λ_i is given by

$$\lambda_i\left(T, \mu\right) = \exp\left(\frac{B_i \mu_B + S_i \mu_S + Q_i \mu_Q}{T}\right) \tag{2.4}$$

and $E_i = \sqrt{p^2 + m_i^2}$ is the energy of particle i.

In the Boltzmann limit, the partition function becomes

$$Z_i = \exp\left[g_i V \int \frac{d^3p}{(2\pi)^3} \lambda_i e^{-(E_i/T)}\right] \tag{2.5}$$

so that the average number of particles of species i is given by

$$\bar{N}_i = \lambda_i \frac{\partial}{\partial \lambda_i} \ln Z_{GC} = g_i \frac{V}{2\pi^2} \int_0^\infty dp p^2 \left[\lambda_i e^{E_i}\right]. \tag{2.6}$$

Boltzmann statistics is appropriate for sufficiently high temperatures with the exception of pions. At high temperatures, the pion multiplicity is very large and has to be handled with Bose-Einstein statistics.

2.3 Particle Multiplicities

Particle abundances are important in that they allow us to infer details of chemical freeze-out in relativistic heavy ion collisions. It has been verified extensively that many particle abundances at the final state of high energy collisions can be described by distributions predicted by thermal models [26, 29, 30]. In doing so, many experimental observables can be reproduced knowing only three parameters. These parameters being temperature T, baryonic chemical potential μ_B and a factor γ_S [31] which accounts for the experimentally observed undersaturation in strangeness. Strictly speaking the only parameters required for a purely statistical approach are T and μ_B. Agreement between the model (with

University of Cape Town

only these parameters) and experimental data would indicate complete chemical equilibrium. Agreement in the case of the inclusion of γ_S would indicate explicit deviation from chemical equilibrium with regards to strangeness.

In general, values inferred with respect to chemical freeze-out are quite sensitive to underlying dynamics. Using ratios of integrated particle yields minimizes the dependence of the model on freeze-out parameters. This is due to the Lorentz invariance of these ratios.

Within the thermal model, particle number densities n_i are determined using statistical distributions. The subscript i indicates a specific hadron type like K^+, π^+, Λ, etc. Using a grand canonical description together with Boltzmann statistics, the thermal particle number densities are given as

$$n_i^0 = g_i \int \frac{d^3p}{(2\pi)^3} \gamma_S^{|S_i|} \lambda_i e^{-(E_i)/T} \tag{2.7}$$

The above expression holds for particles inside a fireball at rest at equilibrium temperature T and the characteristic chemical potentials for particle species i having baryon number B_i, strangeness S_i and electric charge Q_i (μ_B, μ_S and μ_Q respectively).

When considering particles with non-zero strangeness, $\gamma_s^{S_i}$ accounts for the deviation in their abundances from equilibrium. For example, on selecting a suitable γ_S for the K^+ ($S = 1$), Ξ^- ($S = -2$), Ω^- ($S = -3$), this factor becomes γ_S^1, γ_S^2, γ_S^3 respectively. However, for particles with hidden strangeness such as the Φ ($s\bar{s}$) or the η ($\frac{u\bar{u}+d\bar{d}-2s\bar{s}}{\sqrt{6}}$), with zero net strangeness, it is still necessary to implement strangeness suppression and with the above prescription, it is not possible. An alternative is described in [32]. Here, if a mass cut off on included resonances of 1.8 GeV is imposed, then the production of neutral hadrons with fraction f of $s\bar{s}$ content is suppressed by a factor $(1 - f) + f\gamma_S^2$. If however, a mass cut-off of 2.4 GeV is imposed then the neutral resonances are suppressed by a factor γ_S^{2f}. Both these treatments have been found to give similar results [32].

Final particle densities also include a contribution from the feed down of the decay

University of Cape Town

from heavier resonances according to their experimentally determined branching ratios (Br). So final particle densities are given by the thermal contribution as in equation 2.1 as well as a the contribution resulting from feed down. For example, the final K^+ number density is given by

$$n_{K^+} = \sum_i n_i Br(i \rightarrow K^+). \tag{2.8}$$

For calculations, all observed resonances up to mass 2 GeV are included. In the thermal model, higher mass resonance contributions are highly suppressed by the Boltzmann factor. In calculating particle ratios, it suffices to take ratios of the relevant particle densities as calculated using the above description.

The procedure described above does not account for the fact that in reality, there is a limit on the density to which a nucleon system can be compressed. This is a valid approximation for small baryon density n_B. There is however a strong short range repulsion between baryons which cannot be ignored for large n_B. Using a hard sphere picture [33], one introduces an intrinsic hard core volume V_0 for the the nucleons in the system, the result being that the available volume V is reduced by $V - NV_0$. Calling the baryon density in a system of point-like nucleons n_B^0 and n_B in a system of nucleons with hard core volume, this means

$$n_B^0 = \frac{N}{V - NV_0} = \frac{n_B}{1 - n_B V_0} \tag{2.9}$$

i.e.

$$n_B = \frac{n_B^0}{1 + n_B^0 V_0} \tag{2.10}$$

where n_B^0 is the density calculated for an ideal gas of point-like baryons (as in equation 2.4). The baryons in the system remove a portion of the available spatial volume. For several baryon species $i = 1, 2, ...K$ the resulting baryon density would be

$$n_B = \frac{n_B^0}{[1 + \sum_{i=1}^{K} V_i n_i^0]} \tag{2.11}$$

One universal volume $V = 4\pi R^3/3$ is chosen for the effective hard sphere volume

University of Cape Town

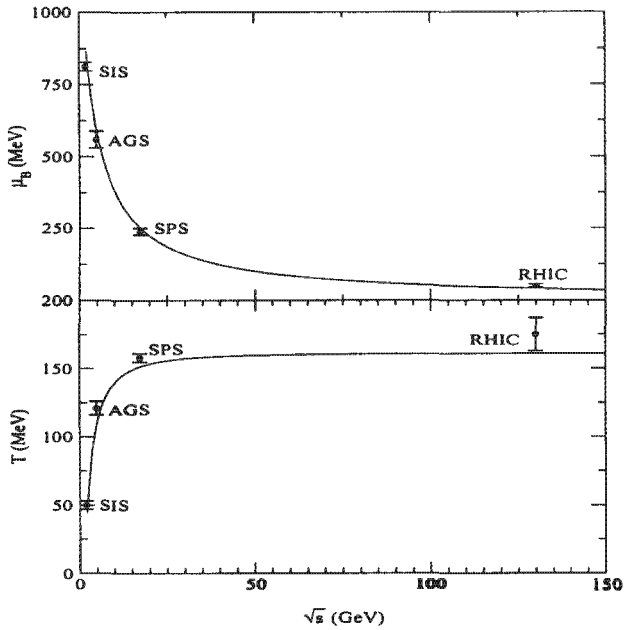

Figure 2.1: Dependence of temperature and baryon chemical potential on center of mass energy [36].

of a nucleon where $R = 0.8fm$ is taken as the approximate radius for a nucleon [33]. This volume correction applies to mesons as well as baryons. In the calculation of particle ratios, this volume correction conveniently cancels out.

Since ordinary matter is neutral with respect to strangeness, the overall strangeness number density for the colliding system $n_S = 0$. Knowing this μ_S can be fixed. For the colliding nuclei, the overall baryon number to charge ratio for a specific system of colliding nuclei is known. This enables μ_Q to be fixed also. Particle number densities can now be expressed in terms of the remaining free parameters T and μ_B.

2.4 Chemical freeze-out parameters

The parameters T and μ_B are determined by examining fully integrated experimental particle yields. Particle yields depend on these parameters. Below the

University of Cape Town

chemical freeze-out temperature, inelastic collisions are no longer important and the abundance of hadrons is fixed.

The values of μ_B at SIS, AGS and SPS energies were extracted from the analysis of the particle multiplicity data [34, 35]. At low beam energies, a hadronic gas is created with low T and high μ_B. This means that the gas is made up predominantly of nucleons and few mesons. As the energy increases, T increases, with corresponding decrease in μ_B. At the high energy side (at RHIC for instance where $\sqrt{s} = 130GeV$), the conditions of high T and low μ_B reflects that the system now consists predominantly of mesons and relatively fewer baryons. From this, the dependence of μ_B on center of mass energy $\sqrt{s}$ can be parameterized. This parameterization [36] is given by

$$\mu_B \simeq \frac{a}{1 + \sqrt{s}/b} \tag{2.12}$$

where $a \simeq 1.27\ GeV$ and $b \simeq 3.3\ GeV$ are determined from the fit. This parameterization is shown graphically in the upper part of figure 2.1.

In spite of the large variation in center of mass energy in the range from SIS to RHIC (which corresponds to more than 100-fold increase), also considering that collisions of different nuclei take place, the average energy per hadron always has a value close to 1 GeV. A non-relativistic interpretation [37] of this is as follows: Non relativistically the average energy per hadron can be given by:

$$\frac{\langle E \rangle}{\langle N \rangle} \simeq \langle M \rangle + \frac{3}{2}T \simeq 1GeV. \tag{2.13}$$

This appears to be valid for low temperatures. For low temperatures, the hadron gas is made up predominantly of nucleons so the average mass for low temperatures would correspond to the nucleon mass m_N.

The unusual observation $\langle E \rangle / \langle N \rangle \simeq 1GeV$ leads to a relation between temperature and baryon chemical potential (shown in figure 2.3) which in turn provides the temperature dependence on center of mass energy. This is shown in the lower part of figure 2.1. Alternatively, this relation, together with only one measured particle ratio can provide the energy dependence of both T and μ_B.

University of Cape Town

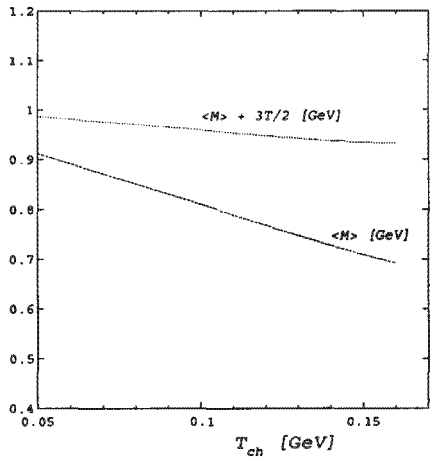

Figure 2.2: Average mass at chemical freeze-out as a function of chemical freeze-out temperature [37].

2.5 Strange to non-strange particle ratios

The role of strangeness in heavy ion collisions (as introduced in chapter 1) has provided much insight into fundamental processes. Strangeness very likely could still hold many surprises. Particularly when considering the relative abundance of strange to non strange particles expected to be produced. As mentioned before, a characteristic non-monotonic dependence of strange to non strange particle ratios on beam energy has been observed experimentally.

2.5.1 The Wroblewski ratio

A useful quantity which enables one to investigate the behavior of total relative strangeness in various systems is the Wroblewski ratio λ_S [39]. It compares the number of newly produced $s\bar{s}$ pairs to all the newly produced $u\bar{u}$ and $d\bar{d}$ light quark pairs i. e.

$$\lambda_S = \frac{2\langle s\bar{s}\rangle}{\langle u\bar{u}\rangle + \langle d\bar{d}\rangle} \tag{2.14}$$

University of Cape Town

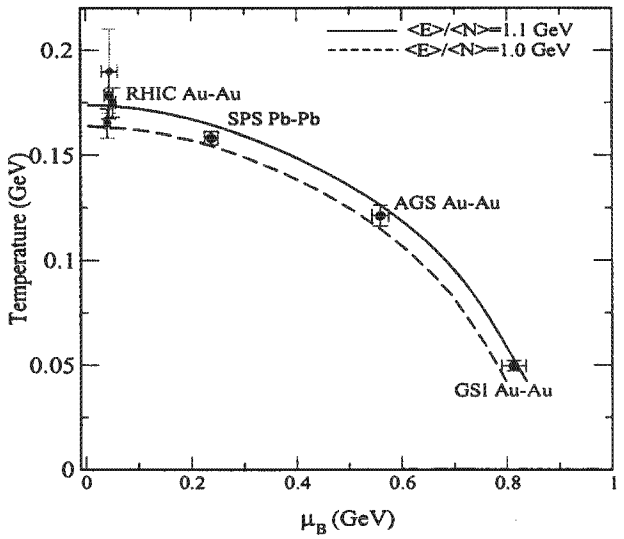

Figure 2.3: Values of temperature and baryon chemical potential at various energies [38].

The Wroblewski ratio excludes all quark pairs originally present in the target and projectile nucleons. The quark content in the Wroblewski ratio is determined from the hadrons and hadronic resonances before they decay (i.e. at chemical freeze-out). This quantity is not easily measurable since it is not a trivial matter to reconstruct all resonances from final state particles.

2.5.2 Maximum in relative strangeness

The observation of non-monotonic energy dependence of $\langle K \rangle^+ / \langle \pi^+ \rangle$ ratio in central $Pb + Pb$ collisions by NA49 motivated the study of energy dependence of strange hadron production within the thermal model [40]. In fact, the non-monotonic dependence has been predicted within the thermal model for several strange hadronic ratios as well as the Wroblewski ratio.

From figure 2.4 it is clear that around 30 $A \cdot GeV$ lab energy, the Wroblewski reaches a maximum [41]. In figure 2.5, one sees that the enhancement contribution of the strange baryons to the Wroblewski ratio before 30 $A \cdot GeV$ lab energy is the origin of the maximum in the Wroblewski ratio. The maximum can be traced to the dependence of mu_B on beam energy. When λ_S is calculated with

University of Cape Town

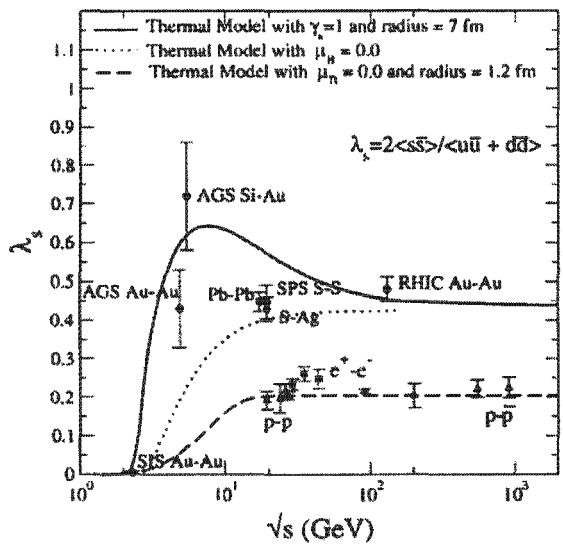

Figure 2.4: The Wroblewski ratio as a function of beam energy [26].

varying temperature and baryon chemical potential fixed at zero, it is found to be a smooth function of energy (shown by the dotted and dashed lines in figure 2.4). This is a close approximation to the situation in elementary particle collisions. One sees that the $p-p$ and $e+e$ data fits the this thermal model approximation well.

Experimentally, the Λ/π^+, K^+/π^+ and Ξ/π^+ ratios all show a maximum with respect to beam energy. This can be seen in figures 2.6 and 3.5. It is important to note that the K^-/π^+ ratio does not reach a maximum. Within the thermal model, this is explained considering the relation between T and μ_B. As collision energy increases, T increases and μ_B decreases correspondingly. This results in an increase of anti-strange baryon yields. By conservation of strangeness, fewer K^+ mesons will be produced and this is what results in the predicted maximum in the K^+/π^+ in the thermal model.

The thermal model reproduces the non-monotonic behavior well for the Λ/π^+ ratio. However, the most recent NA49 data shows a sharp spike in the 4π inte-

University of Cape Town

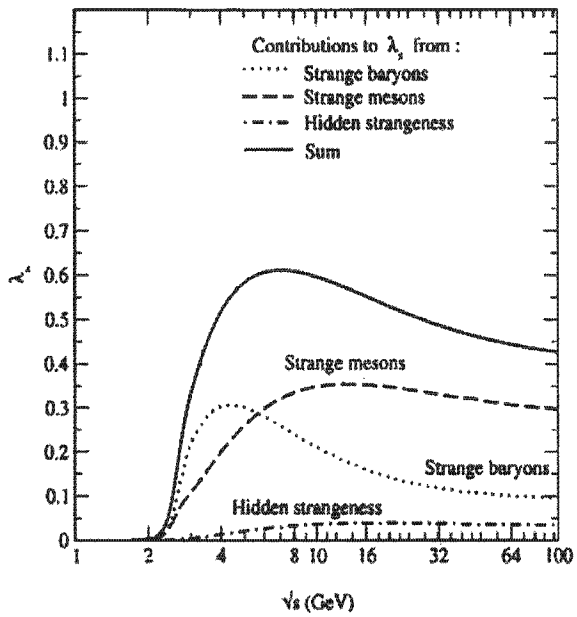

Figure 2.5: Contributions to the Wroblewski ratio from strange baryons, strange mesons and particles with hidden strangeness [26].

grated K^+/π^+ ratio. This is not reproducible in the thermal model. The thermal model predicts smooth behavior and a broad maximum for this ratio. The deviation from the thermal model prediction could be interpreted as indicating the presence of new dynamics. The statistical model of the early stages (see chapter 3) might potentially provide a better description of this ratio. From figure 2.6, we see that the Λ/π^+ peak is more pronounced than the Ξ^-/π^+ peak which in turn is more pronounced than the Ω/π^+ peak. This is expected since an increase in the strangeness content of a particle should suppress it's dependence on μ_B.

2.5.3 Contours in fixed strange to non strange particle ratios

By scanning over a wide range of values of T and μ_B, and calculating a specific particle ratio for each pair of parameters, one can gain a better understanding of the features of the thermal mode. Comparing these results to those obtained using the experimentally extracted parameters could also provide insight into experimentally observed chemical freeze-out. Such scans were performed for the

University of Cape Town

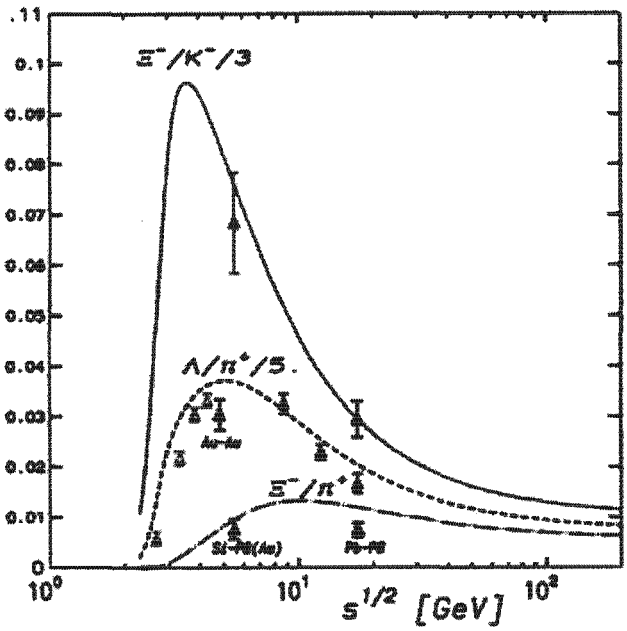

Figure 2.6: Prediction for the ratios Λ/π^+, Ξ^-/π^+ and Ω^-/π^+ as a function of center of mass energy $\sqrt{s}$ [36].

ratios discussed above. In these calculations, the strangeness saturation factor γ_S was set to 1 (assumption of fully equilibrated strangeness), μ_S was constrained by setting the overall strangeness to zero, and the electric charge chemical potential μ_Q was constrained by setting the baryon to charge ratio $B/2Q = 1.2683$ (a $Pb + Pb$ system). The result of this is shown in figures 2.7, 2.8, 2.9 and 2.10 for the K^+/π^+, Λ/π^+, Ξ^-/π^+ and Ω^-/π^+ ratios respectively.

One observes from these plots that a fixed particle ratio corresponds to a contour in the T, μ_B plane. The appearance of closed contours seems to be unique to particle ratios which reach a maximum. The particle ratio becomes progressively larger until the maximum in the ratio is reached (the innermost contour). Each contour characterizes a unique relationship between T and μ_B for a specific value of a particle ratio.

For the Λ/π^+ contour for instance, following a contour, it is apparent that a specific ratio is produced along a contour where T varies dramatically with very little variation in μ_B. For approximately half of the contour, T increases while

University of Cape Town

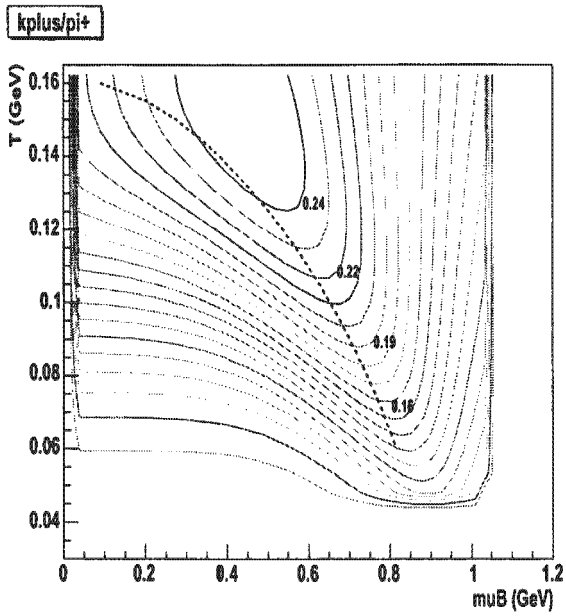

Figure 2.7: Contours of constant particle ratio (K^+/π^+) in the T, μ_B plane superimposed on the universal freeze-out curve.

μ_B decreases. On the other half, T decreases while μ_B increases. If one draws an axis through the turning points of the contours, this relationship appears to be symmetric with respect to the axis. This is true for the strange baryon ratios calculated (Λ/π^+ and Ξ^-/π^+). This symmetry is not present in the K^+/π^+ ratio. For this ratio, if one draws an axis through the turning points of the contours, the segment of the contour below the axis shows a far larger variation in μ_B with changing T.

Surprising features appear when looking at the contours in relation to the freeze-out curve. The maxima lie in close proximity to the freeze-out curve. It is therefore sensible to speculate that there is a relation between the appearance of the maxima in particle ratios and experimentally observed chemical freeze-out conditions. If one looks at the position of the maxima of the strange baryons with respect to the freeze-out curve, it is evident that the position of the maxima with respect to T and μ_B is dependent on the amount of strange quarks present in the baryon. The more strange quarks present in the baryon, the lower the maximum appears with respect to μ_B, and the higher it appears with respect to T.

University of Cape Town

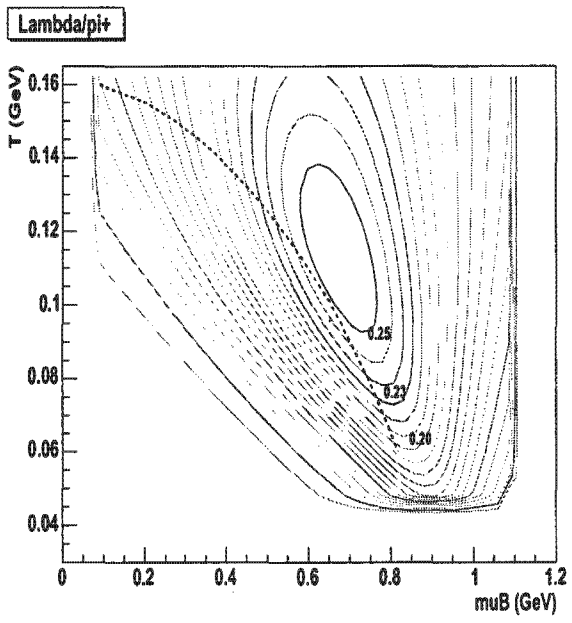

Figure 2.8: Contours of constant particle ratio (Λ^+/π^+) in the T, μ_B plane superimposed on the universal freeze-out curve.

In addition, it appears that the turning points (minimum in T) of the contours are also related to experimental chemical freeze-out since the freeze-out curve intersects the contours very near to their turning points. This happens almost exactly for the Λ/π^+ and K^+/π^+ contours. As the freeze-out curve approaches the maximum, deviation it moves away from the turning points.

It is important to not that the contours are purely a feature of the thermal model. The particle ratios are calculated without assuming the experimental relation between T and μ_B. Thus there is no reason to expect that the maximum value calculated for a specific ratio should occur at a T, μ_B pair lying along the freeze-out curve. The fact that the maxima in the above strange to non strange particle ratios do indeed lie close to the freeze-out curve indicates that there is a link between the maximum in strangeness (predicted by the thermal model) and experimentally observed chemical freeze-out. Understanding why this happens requires a more qualitative meaning of the condition $E/N = 1$ in terms of the thermal model.

University of Cape Town

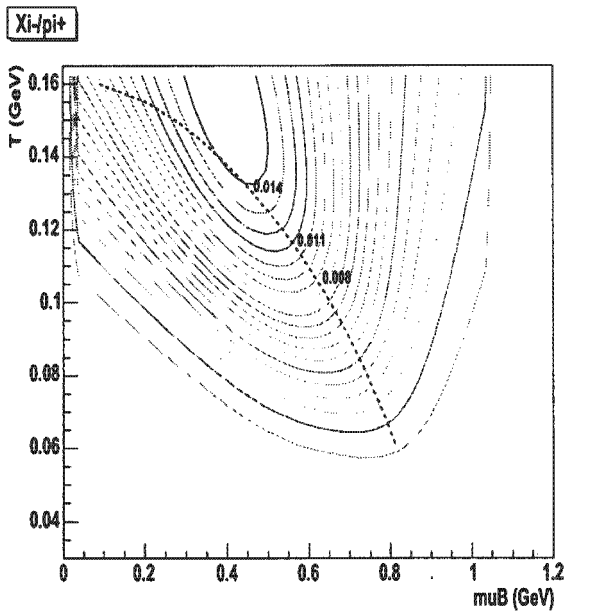

Figure 2.9: Contours of constant particle ratio (Ξ^-/π^+) in the T, μ_B plane superimposed on the universal freeze-out curve.

It is interesting also that the freeze-out curve runs through the turning points of the contours. It is possible that this phenomenon is indicative of a more general relationship between chemical freeze-out and strangeness calculated in the thermal model. The proximity of the maxima in strange to non strange hadronic ratios to the freeze-out curve might possibly be limiting behavior of this relation.

University of Cape Town

2.5.4 The Λ/π^+ ratio in more detail

From the previous contour plots, it is evident that although the maxima in strange to non strange particle ratios calculated in the thermal model all lie close to the freeze-out curve, they do not appear at the same T and μ_B. In order to check whether the mass is the factor determining the position of the maxima, I varied the mass of the Λ in small increments from it's known mass of 1.116 GeV to 1.40 GeV and produced a contour plot of the Λ/π^+ ratio for each mass. The result of this is shown in the series of plots presented in figures 2.11 to 2.14.

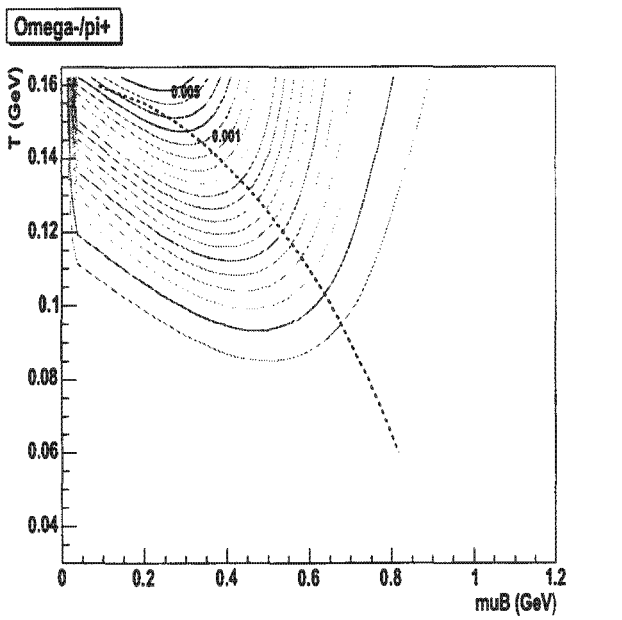

Figure 2.10: Contours of constant particle ratio (Ω^-/π^+) in the T, μ_B plane superimposed on the universal freeze-out curve.

The approximate center of the position of the maximum for the calculation with Λ mass $= 1.116\ GeV$ is referenced by a cross in each of the plots. The value of the maximum decreases slightly with increase in the mass of the Λ. The decrease is so slight that one could conclude that the value of the maximum is almost independent on the mass of the Λ. Also the position of the maxima appears to remain almost fixed with respect to μ_B but shifted to a higher T for higher mass. This is not unexpected because higher mass resonances require higher temperatures to be produced. Note that the dimensions of the contours with respect to T and μ_B do not change. As a consequence of the increased temperature (but unchanged μ_B) required required to produce a maximum, the maximum moves away from the freeze-out curve as the mass is increased.

University of Cape Town

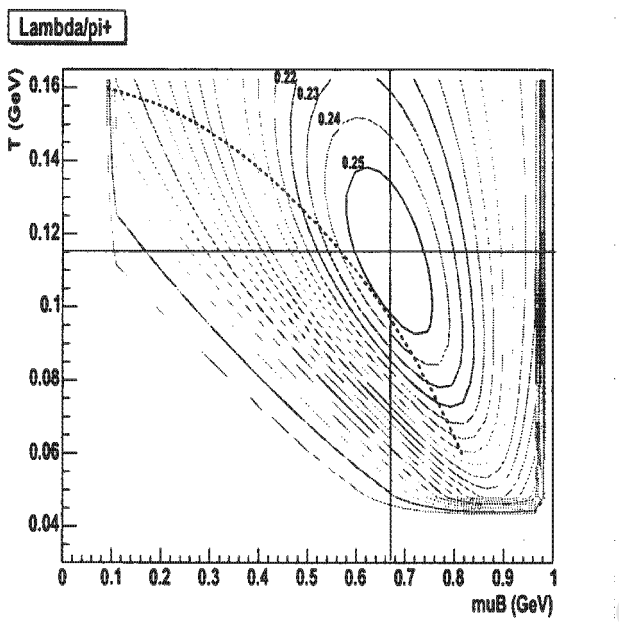

Figure 2.11: Contours in constant Λ/π^+ for Λ mass=1.116 GeV; maximum= 0.250

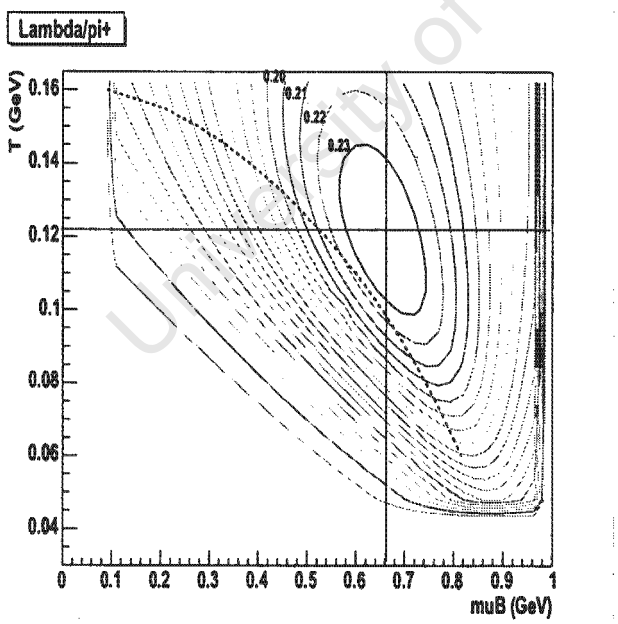

Figure 2.12: Contours in constant Λ/π^+ for Λ mass=1.15 GeV maximum= 0.230

University of Cape Town

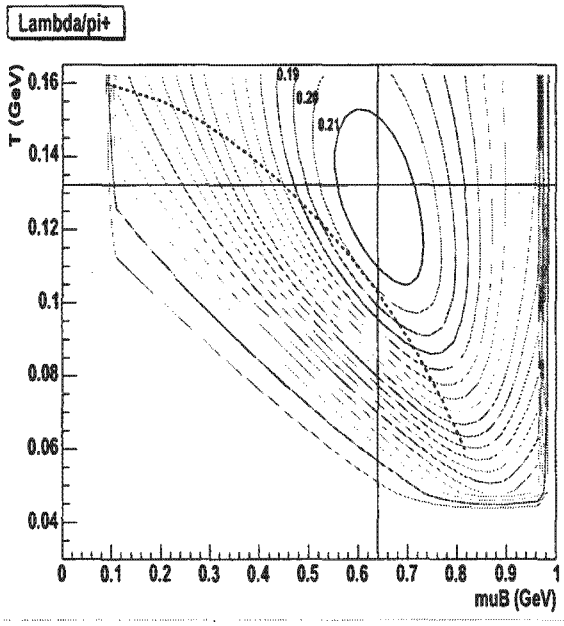

Figure 2.13: Contours in constant Λ/π^+ for Λ mass=1.20 GeV maximum= 0.210

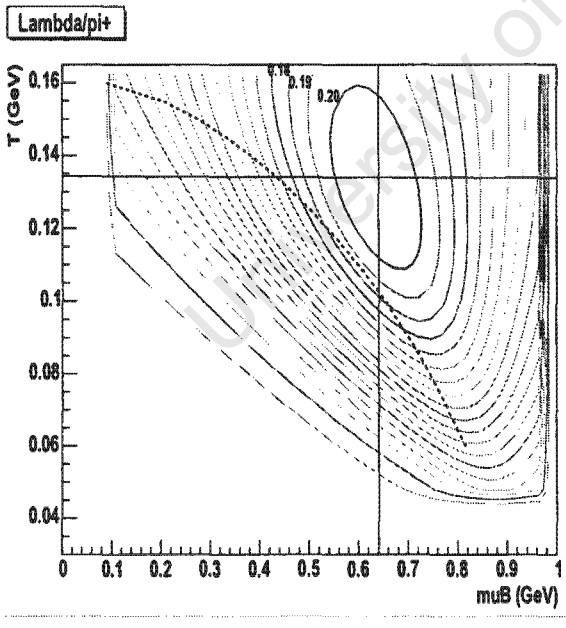

Figure 2.14: Contours in constant Λ/π^+ for Λ mass=1.25 GeV maximum= 0.200

University of Cape Town

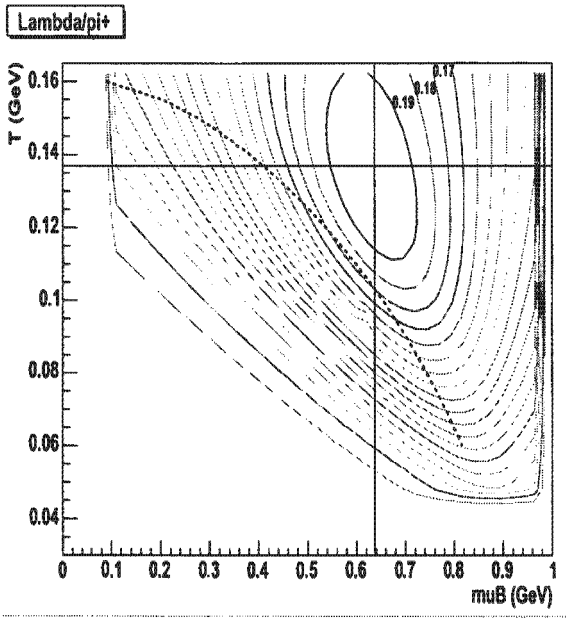

Figure 2.15: Contours in constant Λ/π^+ for Λ mass=1.30 GeV maximum= 0.190

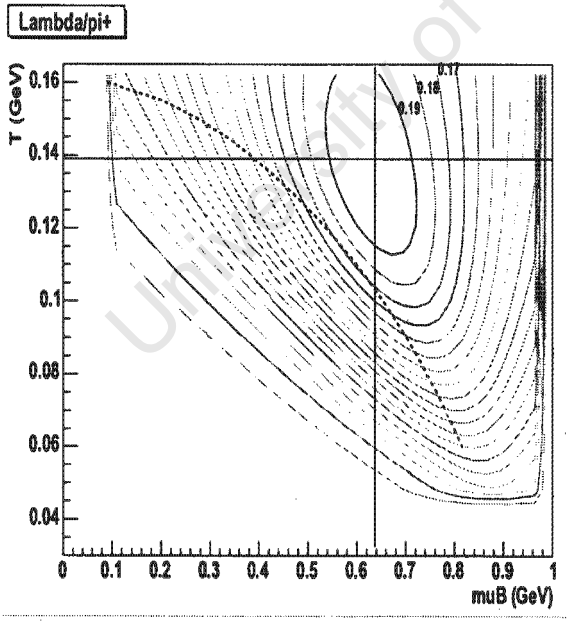

Figure 2.16: Contours in constant Λ/π^+ for Λ mass=1.35 GeV maximum= 0.190

University of Cape Town

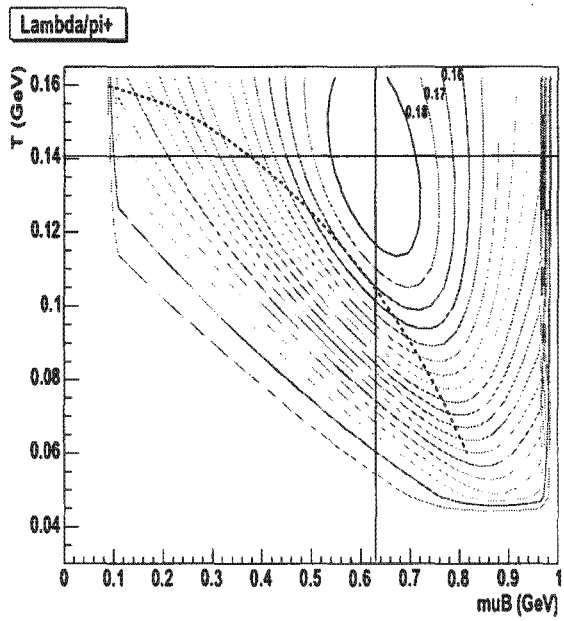

Figure 2.17: Contours in constant Λ/π^+ for Λ mass=1.40 GeV maximum= 0.180

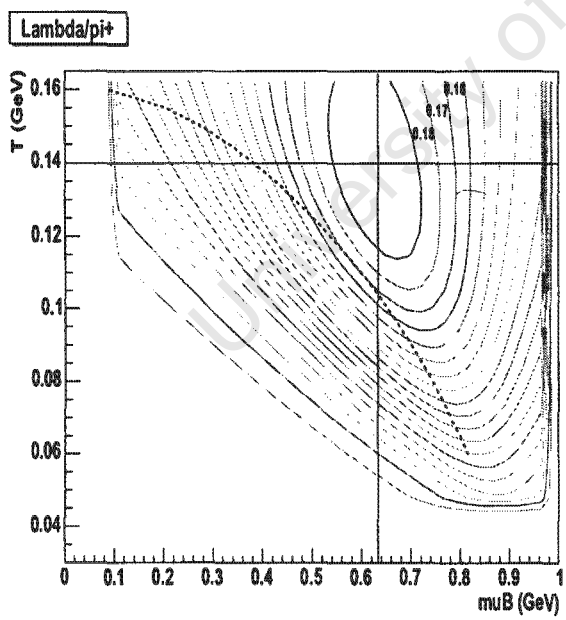

Figure 2.18: Contours in constant Λ/π^+ for Λ mass=1.45 GeV maximum= 0.180

University of Cape Town

Chapter 3

Statistical Model of the Early Stages

University of Cape Town

3.1 Overview of the model

This phenomenological model was developed by Gaździcki and Gorenstein [42]. It models the early stages of nucleus-nucleus collisions so that its properties can be understood. The model relies on the assumption that entropy and heavy flavors are insensitive to the late stages of the collision and consequently, would carry information about the early stages where insensitive quantities would be reflected in the experimentally observed properties of the gas of hadrons.

As mentioned before it is widely accepted that a high enough collision energy density might lead to the formation of a state in which the effective degrees are quarks and gluons (QGP) (also referred to in the model as a Q-state). The standard model of particle physics allows one to determine the number of degrees of freedom in a state where the quarks and gluons are deconfined in relatively simple and manner. Consequently, describing this state within the model is neatly done.

For collisions in which energy densities are not high enough for the formation of a deconfined Q state (within the framework of the model) the description is less quantitative. Rather than describe the early stage as a gas of hadrons and hadronic resonances, the confined early state assumed is one in which the effective

degrees of freedom are point-like colorless bosons (pions and kaons). This state is referred to as as a white (W) state. This was motivated by the understanding of $e^+ + e^-$ annihilation process in which the degrees of freedom are found experimentally to be colorless $q\bar{q}$ pairs [43]. The properties of this state is described by an effective parameterization.

The basic assumption of the model is that the production of new degrees of freedom is a statistical process. Only states with net baryon number, flavor and electric charge = 0 are possible (particle creation obeys baryon, flavor and electric charge conservation). Since overall baryon number must be conserved during the collision, part of the total energy has to be carried by the net baryons. The remainder of the energy available for particle creation is expressed as

$$E = \eta(\sqrt{s_{NN}} - m_N)A_p \tag{3.1}$$

where $\sqrt{s_{NN}}$ is the energy in the center of mass system, m_N is the nucleon mass, A_p is the number of participant nucleons from one nucleus and η is the fraction of energy available for the production process.

Using a grand canonical partition function the ideal gas pressure is written as

$$p^i(T) = \frac{g^i}{2\pi^2}\int_0^\infty k^2 dk \frac{k^2}{3\left(k^2+m_i^2\right)^{\frac{1}{2}}} \frac{1}{exp\left(\frac{\sqrt{k^2+m_i^2}}{T}\right) \pm 1} \tag{3.2}$$

where g^i is the number of internal degrees of freedom for particle species j , m_j is the particle mass and $-$ refers to bosons and the $+$ to fermions. Given the pressure, energy density ε and entropy density s are simply

$$s = \frac{dp}{dT} \tag{3.3}$$

and

$$\varepsilon = T\frac{dp}{dT} - p \tag{3.4}$$

Within the model, an ideal gas description of the W-state (as above) is assumed. For the creation of quarks and gluons (or the Q state), the strong interaction between the quarks and gluons and the surrounding vacuum is accounted for by

University of Cape Town

introducing a bag constant B into the equation of state as follows [44, 45]

$$p = p^{id} - B. \tag{3.5}$$

Because of the assumption that the formation of new degrees of freedom is statistical, the early state is formed in equilibrium. In contrast to the thermal model, equilibration is not due to secondary rescattering. The state of maximum entropy state is the equilibrium state and may be a pure Q, pure W or a mixture of a Q and W state. In the mixed state region, the maximum entropy state changes with the collision energy. Hadronization occurs when the early

3.2 Application of the model

The number density for particle species i is obtained from equation 2.6. In the thermal model, number densities were calculated for hadrons assuming the conditions of a hadron gas in chemical equilibrium. Modeling the early stages however, the input to equation 2.6 would be early stage temperature T, the number of degrees of freedom g_i (depending on whether a Q-state or W-state was formed) for particle species i with mass m_i.

3.2.1 Degrees of freedom and their mass

• **Q-state**

Degrees of freedom in the Q-state are assumed to be quarks and gluons. Non strange degrees of freedom are massless u ($\bar{u}$) quark, d ($\bar{d}$) quarks and the gluon. The strange degree of freedom in this state is taken to be the s quark with mass $= 175\ MeV$. Each quark has 6 internal degrees of freedom (3 color states $\times$ 2 spin states) and each gluon has 16 (8 color states $\times$ 2 spin states). Since the u ($\bar{u}$) and d ($\bar{d}$) quarks are taken to be massless, the effective number of non strange degrees of freedom in the Q-state is given by $g_{gluons} + \frac{7}{8} g_{quarks} = 2 \cdot 8 + \frac{7}{8} \cdot 2 \cdot 2 \cdot 3 \cdot 2 = 37$. The number of strange degrees of freedom in the Q-state is $2 \cdot 2 \cdot 3 = 12$.

• **W-state**

There is no clear way to determine the number of degrees of freedom for a W-state. The non strange degrees of freedom in this state are also taken to be

University of Cape Town

massless while the strange degree of freedom is assumed to have a mass of 500 MeV (kaon mass).

Fitting internal degrees of freedom for data from $N+N$ and $A+A$ data [46, 47], the internal number of degrees of freedom was found to be 3 times lower than found for SPS $A+A$ collisions (where the model assumes the creation of a QGP). In a QGP with all degrees of freedom being massless, the total internal of degrees of freedom $= 16 + \frac{7}{8} \cdot 36 \simeq 48$. The (massless) non strange degrees of freedom in a W-state was therefore taken to be 16 (3 times lower than the internal degrees of freedom in a QGP).

Fitting the strangeness to pion data at the AGS indicated that the strange degrees of freedom in the W-state was 14.

University of Cape Town

3.2.2 Early stage temperature

The early stage temperature can be found within the model by considering the early stage energy density. Within the model the early stage energy density is

$$\varepsilon = \frac{E}{V} \tag{3.6}$$

where E is the energy available for production of particles (as in equation 3.1) and V is the Lorentz contracted volume (which the participating nucleons from a single nucleus occupy)given by

$$V = \frac{\frac{4}{3}\pi r_0^3 A_p}{\gamma} \tag{3.7}$$

where $\gamma = \sqrt{s_{NN}}/2m_N$. By fitting the mean baryon density in the nucleus ($\rho_0 = 0.11 fm^{-3}$), r_0 is estimated as $1.30 fm$.

The energy density can therefore be written as

$$\varepsilon = \frac{\eta\rho_0 \left(\sqrt{s_{NN}} - 2m_N\right)\sqrt{s_{NN}}}{2m_N}. \tag{3.8}$$

Assuming a first order phase transition at $T_c = 200\ MeV$, it follows that: $\sqrt{s_{NN}} < 7.6\ GeV$ is the region in which the confined W-state exists, $7.6\ GeV < \sqrt{s_{NN}} < 10.7\ GeV$ is the phase transition region while $\sqrt{s_{NN}} \gtrsim 10.7\ GeV$ is the QGP region.

In the region of the phase transition, the early stage temperature is constant at approximately 200 MeV. The analysis of hadron multiplicities in $A+A$ collisions at SPS indicate hadron chemical freeze-out to occur at a temperature of 160-190 MeV [48, 49, 50, 51, 52]. The phase transition temperature is in effect chosen as an upper limit to hadron freeze-out temperature. This phase transition temperature corresponds to a bag constant B of 600 MeV/fm^{-3}.

Early stage temperature is shown in figure 3.1 as a function of the energy measure F [53, 54] defined as

$$F = \frac{\left(\sqrt{s_{NN}} - 2m_N\right)^{\frac{3}{4}}}{\left(\sqrt{s_{NN}}\right)^{\frac{1}{4}}} \tag{3.9}$$

F is significant in that the pion yield appears to be proportional to it. For comparison, on the right hand side of figure 3.1 is the early stage temperature as a function of collision energy $(\sqrt{s_{NN}})$.

University of Cape Town

3.2.3 Entropy

Pions are by far the dominant particle species produced in heavy ion collisions and are for this reason interpreted in the model as the ideal tool for studying the entropy which is created in the collision of heavy ions. Because the number of degrees of freedom in a Q-state is much higher than that of a W-state, the entropy is expected to be significantly larger in the event of QGP creation.

For the comparison of the SMES prediction of entropy with experiment, the following quantity is defined:

$$\langle S_\pi \rangle = \langle \pi \rangle + \kappa \left\langle K + \bar{K} \right\rangle + \alpha \langle N_p \rangle . \tag{3.10}$$

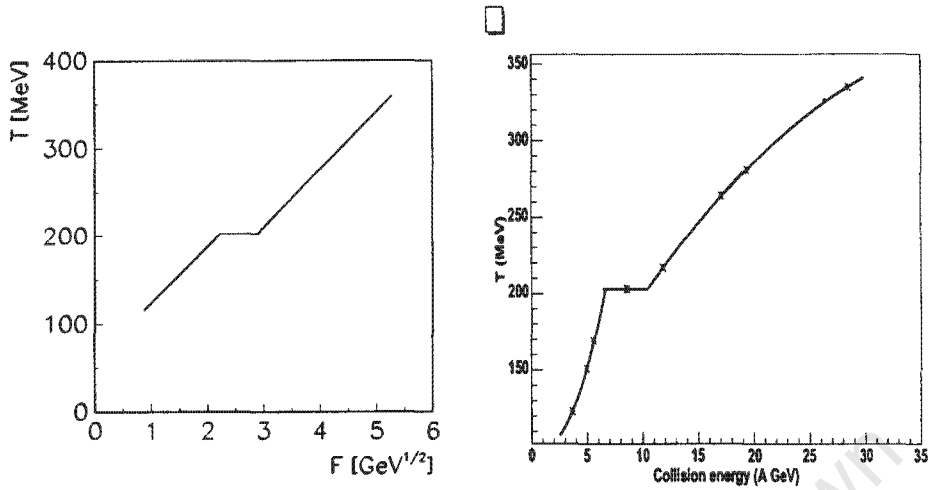

Figure 3.1: The early stage temperature as a function of F [42] (left) and Collision energy (right) in c.m system per nucleon-nucleon pair.

The measured multiplicity of pions is $\langle \pi \rangle$ and the multiplicity of kaons and antikaons is $\left\langle K + \bar{K} \right\rangle$. The factor κ is the ratio of the mean entropy carried by a single kaon to the corresponding pion entropy at chemical freeze-out ($\kappa \simeq 1.6$). The factor $\alpha = 0.35$ makes allowance for the transfer of entropy to baryons. The experimentally determined number of participating nucleons $\langle N_P \rangle$ corresponds to the number of baryons participating in the collisions, $(2A_p)$. Within the model, $\langle S_\pi \rangle$ is interpreted as the *early stage* entropy in units of pion entropy. This appears to assume that the entropy carried by pions and kaons does not change from the early stages to chemical freeze-out. Entropy $\langle S \rangle$ is taken to be 4 times larger than $\langle S_\pi \rangle$ [42]. In the thermal model, the partition function describing the final state is taken to be the sum of the partition function of all hadrons and hadronic resonances present. Thus when calculating entropy in the thermal model, the partition functions of all known resonances is taken into account. In SMES, entropy can inferred from S_π by observing how experimentally observed entropy compares to S_π.

Figure 3.2 shows the comparison of the model prediction for $\langle S_\pi \rangle / \langle N_P \rangle$ as a function of F. The the AGS data has been used to fit the data at low energies while application of the model reproduces the SPS results (where a QGP is as-

University of Cape Town

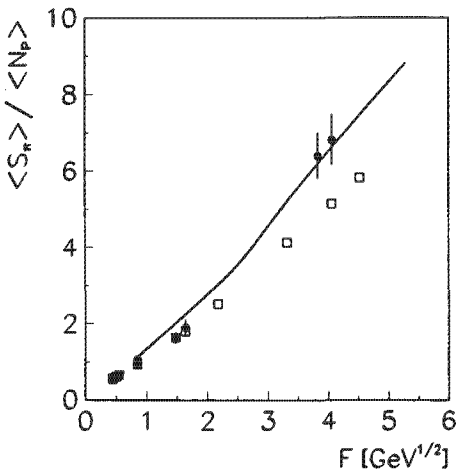

Figure 3.2: $\langle S_\pi \rangle$ / $\langle N_P \rangle$ vs F. Filled circles show data taken from collisions of identical nuclei while open squares indicate data from nucleon-nucleon interactions. [42].

sumed to be created).

Similar behavior is observed in the ratio of total pion multiplicity to the number of wounded (participating) nucleons as shown in figure 3.3. Here the solid line indicates a fit to the data. The increase in the slope (in $A + A$ data) by a factor of $\simeq 1.3$ is interpreted as being caused by the increased number of degrees of freedom as a result of the creation of a QGP [55].

3.3 Maximum in relative strangeness

As mentioned before, heavy flavors and entropy are very important in the model as they are not expected to be altered significantly from the early stages to the time of hadronic freeze-out. It is therefore useful to look at the relative behavior of these two quantities by observing quantities reflecting the ratio of strangeness to entropy.

A variable which enables comparison of the peak in the ratio of strangeness to entropy is defined as follows

University of Cape Town

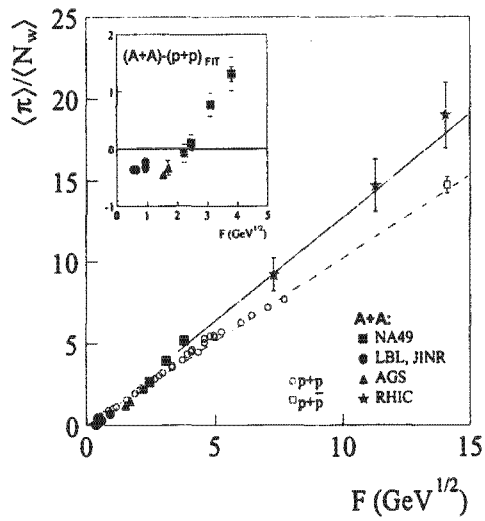

Figure 3.3: Ratio of total pion multiplicity $\langle \pi \rangle$ per wounded (participant) nucleon $\langle N_W \rangle$ as a function of F [55].

$$E_S = \frac{\langle \Lambda \rangle + \left\langle K + \bar{K} \right\rangle}{\langle \pi \rangle}. \tag{3.11}$$

Here $\langle \Lambda \rangle$, $\left\langle K + \bar{K} \right\rangle$ and $\langle \pi \rangle$ are the experimentally measured Λ, summed K and $\bar{K}$ and π yields respectively.

Within the model this quantity is determined as

$$E_s = \frac{(N_s + N_{\bar{s}})/\zeta}{(S - S_s)/4 - \alpha \langle N_P \rangle}. \tag{3.12}$$

The quantity $\zeta = 1.36$ is the experimental ratio of the total strangeness and that carried by Λ's and $(K + \bar{K})$'s. S_s is the proportion of entropy carried by the strangeness carriers (depending on which state was created). The term $\alpha \langle N_p \rangle$ accounts for the entropy transfer to baryons. The denominator thus reflects the entropy carried by pions. Figure 3.4 shows the the comparison of the experimentally determined E_s to the model prediction as a function of energy.

Within the model, a sharp maximum in E_S appears as a consequence of the transition from the W-state to the Q-state (quark-gluon plasma). To be more explicit,

University of Cape Town

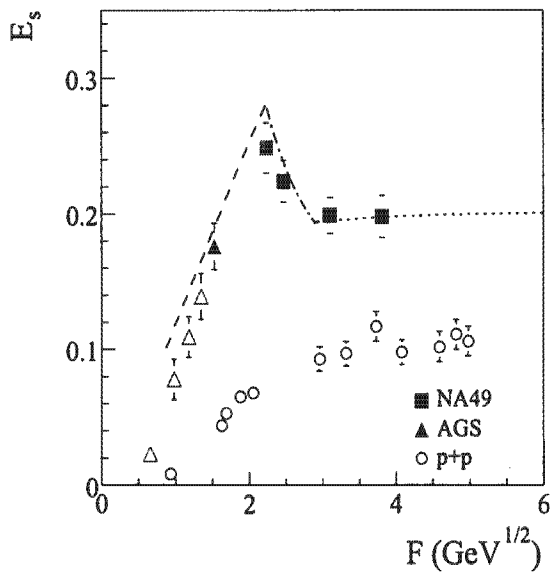

Figure 3.4: The E_s as a function of F [42].

University of Cape Town

for $\sqrt{s_{NN}} < 6.7\ GeV$, strangeness carriers were taken to have 500 MeV mass and the number of strange degrees of freedom was taken to be 16. For $\sqrt{s_{NN}} > 7.6$ GeV the strangeness are s and $\bar{s}$ so that the total number of strange degrees of freedom is 12. With this information, the number of strangeness carriers was calculated in the appropriate energy range. A maximum appears as a result of a significant reduction of the mass of the strangeness carriers and the decrease in the ratio of strange to non-strange degrees of freedom when going from confined (W-state) to deconfined (Q-state) matter.

The SMES provides a remarkable description of the data for E_s. It is however important to remember that the W-state domain is a parameterization so that it is not surprising that in this region the model agrees well with experiment. This low energy parameterization is essential for extrapolation to the transition region. The description of the and higher energy Q-state, where a good agreement between the model and experimental data is once again evident, is independent of the W-state parameterization.

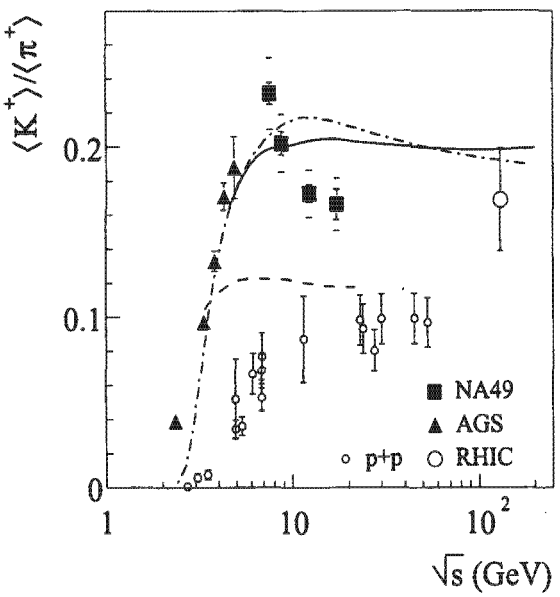

Figure 3.5: The K^+/π^+ ratio as a function of as a function of $\sqrt{s_{NN}}$. The dashed-dotted line indicates the thermal model prediction for this ratio. [56].

Figure 3.5 shows the 4π integrated $\langle K^+ \rangle / \langle \pi^+ \rangle$ ratio as a function of $\sqrt{s_{NN}}$. Here, a sharp peak in the ratio is also observed. However, E_S is shown as a function of F. The relation between F and $\sqrt{s_{NN}}$ (equation 3.10) is not linear. The peak in E_S would appear smoother if shown as a function of $\sqrt{s_{NN}}$. The data would appear more spread out with respect to $\sqrt{s_{NN}}$ especially for $F < 3\ GeV^{1/2}$.

The sharp peak in the data for the $\langle K^+ \rangle / \langle \pi^+ \rangle$ ratio does not resemble the thermal model prediction (as seen in figure 3.3). Because of the successful SMES reproduction of the E_S data, it appears that this model might provide a better description of the experimental behavior. Unfortunately, the SMES is not able to predict particle multiplicities in the hadronic stages from the calculated amount of strangeness carriers in the early stages. Therefore at this stage, one cannot conclude that SMES could provide a description of the $\langle K^+ \rangle / \langle \pi^+ \rangle$ ratio.

University of Cape Town

Chapter 4

Comparison and Discussion of Thermal model and SMES

University of Cape Town

Thermal models basically infer a chemical potential and chemical freeze-out temperature from experimental data to model the final hadronic state using statistical mechanics. Thus thermal models enable one to identify to what extent hadronic systems are equilibrated chemically. Rescattering erases the memory of a thermalized system. Therefore, thermal models alone cannot be used to draw bold conclusions about dynamics at early stages of the evolution of colliding systems.

SMES on the other hand, predicts the change of properties of the early stage of a colliding system as a function of collision energy due to a deconfinement phase transition. The assumption of the transition temperature and properties of confined and deconfined phases determines the energy range in which a transition takes place.

The NA49 data on relative strangeness shows substantial deviation from the smooth behavior predicted by the thermal model. The NA49 4π $\langle K^+ \rangle / \langle \pi^+ \rangle$ data is evidence for this. The SMES description of E_S shows good agreement with the trend observed in the data. It is possible that a SMES description for the $\langle K^+ \rangle / \langle \pi^+ \rangle$ ratio would show satisfactory agreement with the data. The most interesting region lies where the sharp peaks are observed. This is the region of the phase transition and is handled in SMES, by the assumption of the creation of a QGP in the SPS energy range.

The SMES models a confined early W-state merely by parameterization of data. The extent of how this fit is useful lies entirely in speculation about the meaning of the fit parameters. A phase transition from a W-state to a QGP occurs shortly above the AGS energy range, which means that the description in the region of the sharp peaks in the SMES relies heavily on the W-state fit. It is also important to note that, in the SMES, the strangeness is assumed to be in equilibrium and thus defined by the variety of strange quarks and the strange quark mass. It is however very widely accepted that strangeness production is a dynamical process which in QGP is dominated by gluon fusion. The SMES, as a statistical model, does not account for dynamical processes.

The interesting phenomenon of closed contours in T and μ_B observed for strange to non strange particle ratios in the thermal model could hold a very fundamental link to chemical freeze-out freeze-out conditions. An understanding of this relationship should provide a qualitative meaning in terms of statistical mechanics about on chemical freeze-out conditions observed in heavy ion collisions.

University of Cape Town

Bibliography

[1] H. Satz, *The limits of hadron thermodynamics* Invited lecture, CERN May 18 1984, Fortsch. Phys **33** 259 (1985).

[2] M. Stephanov, "QCD Phase diagram and the critical point",hep-ph/0402115 (2004).

[3] S. Slegt *Space-time evolution in relativistic heavy-ion collisions* PhD thesis, Rijksuniversiteit Groningen (1995).

[4] M. Strickland, Phys. Lett. B **331** 245 (1994).

[5] M. Strickland, Phys. Rev. Lett **73** 2421 (1994).

[6] G. Domokos, J. I. Goldman, Phys. Rev. D **23** 203 (1981).

[7] T. Matsui, H. Satz, Phys. Lett. B **178** 416 (1986).

[8] H. Satz, Nucl. Phys. A **418** 447C (1984).

[9] M. H. Thoma, M. Gyulassy, Nucl. Phys. B **351** 491 (1991).

[10] M. Gyulassy, X.-N. Wang, Nucl. Phys. B **420** 583 (1994).

[11] X.-N. Yang, Phys. Lett. B **579** 299 (2004) (nucl-th/0307036).

[12] S. Jeon, V. Koch, Phys. Rev. Lett. **85** 2076 (2000) (hep-ph/0003168). 0

[13] P. Koch, B Müller, J. Rafelski, Z. Phys. A **324** 453 (1986).

[14] J. Rafelski, Phys. Rep **88** 331 (1982).

[15] P. Koch, J. Rafelski, Nucl. Phys. A **444** 678 (1985)

University of Cape Town

[16] P. Koch, B. Müller, J. Rafelski, Phys. Rep. **142** 167 (1986).

[17] J. Rafelski, Jean Letessier, J. Phys. G **30** S1-S28 (2004) (hep-ph/0305284).

[18] J. Castillo, J. Phys G **28** 1987 (2002).

[19] F. Becattini, J. Cleymans, J. Keranen, A. Suhonen, K. Redlich, Phys. Rev. C **64** 024901 (2001).

[20] J. Bartke, et al, Z. Phys. **C48** 181 (1990).

[21] E. Andersen, et al, WA97 Collaboration, Phys. Lett. B **449** 401 (1999).

[22] N. Carrer, NA57 Collaboration, Nucl. Phys. A **698** 29 (2002).

[23] R. Hagedorn, CERN Rep. 71 (1971); E. Shuryak, Phys. Lett. B **42** 357 (1972); J. Rafelski, Phys. Lett. B **97** 279 (1980); R. Hagedorn, etal., Z. Phys. C **27** 541 (1985).

[24] M. Gaździcki *et al* (Na49 Collaboration) these proceedings.

[25] Huan Z. Huang, J. Phys. G **30** S401-S410 (2004).

[26] P. Braun-Munzinger, K. Redlich, J. Stachel *Particle production in heavy ion collisions*, (2003) (nucl-th/0304013).

[27] J. S. Hamieh, K. Redlich, A. Tounsi, Phys. Lett. B **486** 61 (2000)

[28] M. Gaździcki, D. Röhrich, Z. Phys. **C71** 55 (1996).

[29] P. Braun-Munzinger, D. Magestro, K. Redlich, J. Stachel, Phys. Lett **B518** 41 (2001).

[30] D. Magestro, J. Phys. **G28** 1745 (2002).

[31] J. Rafelski, Phys. Lett. **262B** 333 (1991).

[32] F. Becattini, J. Cleymans, A. Keränen, E. Suhonen, K. Redlich, *Features of particle multiplicities and strangeness production in central heavy ion collisions between 1.7 A and 158 A GeV/c.* (2000) (hep-hp/0002267 v3).

[33] J. Cleymans, K. Redlich, H. Satz, E. Suhonen, Z. Phys. **C33** 133 (1986).

University of Cape Town

[34] J. Cleymans, H. Oeschler, K. Redlich, Phys. Rev. (C59)1663 (1999)
J. Cleymans, H. Oeschler, K. Redlich, Phys. Rev. (B 485) 27 (2000).

[35] F. Becattini, J. Cleymans, A. Keränen, E. Suhonen, K. Redlich, Phys. Rev. C **64** 024901 (2001) (hep-ph/0002267).

[36] P. Braun-Munzinger, J. Cleymans, H. Oeschler and K. Redlich, Nuclear Physics A **697** 902 (2002).

[37] J. Cleymans, K. Redlich, Phys. Rev. C **60** (1999), (nucl-th/9903063).

[38] J. Cleymans, J. Phys. G: Nucl. Part. Phys. **28** 1575 (2002).

[39] K. Wroblewski, Acta. Phys. Polon. B **16** 379 (1985).

[40] Krzysztof Redlich, Nucl. Phys. A **698** 94 (2002).

[41] J. Cleymans, Pramana **60** 787 (2003) (hep-ph/0201142 v1).

[42] M. Gaździcki, M.I. Gorenstein, Acta Phys. Polon. **B30**, 2705 (1999).

[43] D. H. Perkins, *Introduction to High Energy Physics* Addison-Wesley Publishing Company (1982).

[44] E. V. Shuryak, Phys. Rev. **61** 71 (1980).

[45] J. Cleymans, R. V. Gavai, E. Suhonen, Phys. Rep. **130** 217 (1986).

[46] M. Gaździcki, Z. Phys. **C66**, 659 (1995).

[47] M. Gaździcki, Z. Phys. **G23**, 1881 (1997) (nucl-th/9706036).

[48] J. Cleymans and H. Satz, Z. Phys. **C57**, 135 (1993), J. Cleymans, K. Redlich, H. Satz and E. Suhonen, Z. Phys. **C58**, 347 (1993) and Nucl. Phys. **A610**, 509 (1996).

[49] P. Braun-Munzinger, J. Stachel, J. P. Wessels and N. Xu, Phys. Lett. B **B365**, 1 (1995), JStachel, Nucl. Phys. **A610**, 509 (1996).

[50] R. A Ritchie, M. I. Gorenstein and H. G. Miller, Z. Phys. **C75**, 535 (1997).

University of Cape Town

[51] F. Becattini, Z. Phys. **C69**, 485 (1996), F. Becattini and U. Heinz, Z. Phys. **C76**, 269 (1997) (hep-ph/9702274).

[52] F. Becattini, M. Gaździcki and J. Sollfrank, Eur. Phys. J. **C5**, 143 (1998).

[53] E. Fermi, Prog. Theor. Phys **5** 570 (1950).

[54] L. D. Landau, Izv. Akad. Nauk SSSR, Ser. Fiz **17** 51 (1953).

[55] M. Gaździcki, J. Phys. G **30** S161-S168 (2003) (hep-ph/0305176).

[56] M. Van Leeuwen *Energy dependence of particle production in nucleus-nucleus collisions at the CERN SPS*, (2003) (nucl-ex/0306004 v1).

University of Cape Town

University of Cape Town